Acta Automatica Sinica
Vol. 34, No. 5 May, 2008
DOI: 10.3724/SP.J.1004.2008.00558



# Acceleration Feedback Enhanced $H_\infty$ Disturbance Attenuation Control for a Class of Nonlinear Underactuated Vehicle Systems

HE Yu-Qing[1, 2] HAN Jian-Da[1]

**Abstract** In this paper, a generalized acceleration feedback control (AFC) design method, named AFC enhanced $H_\infty$ controller, is proposed for both fullactuated and underactuated nonlinear autonomous vehicle systems. The AFC is designed as a robust enhancement to the normal control based on known dynamics. First, in order to reject the uncertainties and external disturbances, a linear prefilter is used in the new AFC design method to replace the high gain in the normal AFC. Then, backstepping algorithm is applied to the AFC design of underactuated systems. The analysis of both the disturbance attenuation in frequency domain and input-output finite gain $L_2$ stability shows the new controller design method is applicable. In the end, simulations are conducted with respect to the tracking control of unmanned model helicopter. The results are compared with those obtained by the tracking control without AFC to verify the feasibility of the new method.

**Key words** Disturbance attenuation, acceleration feedback control, underactuated systems, backstepping, nonlinear $H_\infty$ control

Unmanned vehicles are being anticipated to handle some high-risk tasks that are dangerous or even impossible for humans. The general goal of the autonomous control for unmanned vehicles is to enable these systems to complete tasks with minimal human interventions. Precise tracking control is a key technology for unmanned systems which are widely used in the areas such as satellite clusters, air traffic control, and the U×Vs in battlefield (unmanned ground/surface/air vehicles)[1]. However, there are at least three difficulties or challenges in the tracking control of unmanned vehicles.

1) The dynamics of most unmanned systems are highly nonlinear, time-varying, and coupled, which might be too complicated to be used for controller design. The controller based on a linearized or simplified model might only guarantee a local performance or result in unexpected tracking error because of the model differences.

2) The working environments of unmanned vehicles are usually dynamic, complex, and unstructured, which bring unpredictable disturbances to the control system, for example, the aerodynamics of UAV and the wave/wind for USV.

3) Many unmanned vehicles, such as UAV[2], USV[3−4], and UUV[5] are underactuated, i.e., a system possessing more degrees of freedom than independent control inputs, which might bring more difficulties for its controller design.

Thus, how to overcome the above difficulties and achieve high tracking performance has been one of the main tasks of the autonomous control of unmanned vehicles.

Traditional robust and adaptive control methods for uncertainty and external disturbances suffer from several problems, including conservativeness because of the inaccuracy in the preassumption of uncertainties, online divergence because of unknown external disturbances, and the complication for real-time implementation.

Many researches on the trajectory tracking of underactuated vehicles have been proposed[6], among which backstepping technique sounds as a useful tool with encouraging achievements. In [2] and [7], backstepping method was proposed for the control of a helicopter, where stable controller and good simulation results were obtained. In [3] and [4], Do et al. successfully designed a path following controller for an underactuated ship. In [8−10], backstepping was used to design a stable tracking controller for UUV. However, the technique itself cannot reject disturbances on either model errors or external disturbances well. Most recently, it was combined with some normal robust control schemes[11−14]. Whereas the backstepping-type robust control still has the disadvantages of normal robust control as mentioned above.

With the advantages of simple structure, high robustness, and easy implementation, acceleration feedback control (AFC) has been successfully used for suppressing uncertainties and external disturbances of "fullactuated" nonlinear mechatronic systems[15−19]. The AFC method is a kind of robust enhancement to the normal control schemes, such as PID. However, a great disadvantage is that it still cannot be used in nonlinear and underactuated systems. Besides, because the direct feeding of acceleration measurement into the input force/torque of the system, the normal AFC introduces an algebra loop which results in that the high-gain AFC is difficult to be implemented for real systems[19].

It should be noted that in most mechatronic systems, if the acceleration signals are measurable, so do the disturbance signals. Thus, AFC design is in fact a disturbance attenuation robust control problem with measurable disturbance signals.

In this paper, the normal high-gain AFC is introduced in Section 1. In Section 2, a "prefilter" is designed to obtain a new AFC enhanced robust controller called AFC enhanced $H_\infty$ controller. In Section 3, the new AFC method is used for a class of underactuated systems. In Section 4, the simulation results with respect to an unmanned helicopter model are conducted to verify the feasibility of the new method.

## 1 High gain AFC

Consider the following input affine nonlinear mechatronic system

$$\ddot{\boldsymbol{p}} = f(\boldsymbol{p}, \dot{\boldsymbol{p}}) + g(\boldsymbol{p}, \dot{\boldsymbol{p}})\boldsymbol{u} + \boldsymbol{\Delta} \tag{1}$$

where $\boldsymbol{p} \in \mathbf{R}^n$ and $\boldsymbol{u} \in \mathbf{R}^m$ are the generalized position vector and input vector, respectively; $f(\cdot,\cdot)$ and $g(\cdot,\cdot)$ are smooth nonlinear functions; and $\boldsymbol{\Delta}$ is the external disturbance.

If $m = n$, i.e., for a fullactuated system, the idea of high-

Received November 10, 2006; in revised form December 26, 2007
1. State Key Laboratory of Robotics, Shenyang Institute of Automation, Chinese Academy Sciences, Shenyang 110016, P. R. China
2. Graduate University of Chinese Academy Sciences, Beijing 100080, P. R. China
DOI: 10.3724/SP.J.1004.2008.00558

gain AFC is to design the following controller as in [17]

$$\boldsymbol{u} = -K_a(\ddot{\boldsymbol{p}} - K_1\boldsymbol{p} - K_2\dot{\boldsymbol{p}}) \tag{2}$$

where $K_a$ is the gain matrix, and $K_1$ and $K_2$ are constant matrices such that

$$\begin{bmatrix} 0 & I \\ -K_1 & -K_2 \end{bmatrix}$$

is Hurwitz.

Combining (1) and (2), we have the following equation

$$\begin{aligned}\ddot{\boldsymbol{p}} =& [I + g(\boldsymbol{p},\dot{\boldsymbol{p}})K_a]^{-1}f(\boldsymbol{p},\dot{\boldsymbol{p}}) + [I + g(\boldsymbol{p},\dot{\boldsymbol{p}})K_a]^{-1}\boldsymbol{\Delta}+\\ & [I + g(\boldsymbol{p},\dot{\boldsymbol{p}})K_a]^{-1}g(\boldsymbol{p},\dot{\boldsymbol{p}})K_a(K_1\boldsymbol{p} + K_2\dot{\boldsymbol{p}})\end{aligned} \tag{3}$$

If $K_a$ could be designed to be big enough to satisfy

$$\|g(\boldsymbol{p},\dot{\boldsymbol{p}})K_a\| \gg \max\{\|f(\boldsymbol{p},\dot{\boldsymbol{p}})\|, \|\boldsymbol{\Delta}\|, 1\} \tag{4}$$

Then, the closed loop of (3) can be approximated as

$$\ddot{\boldsymbol{p}} = K_1\boldsymbol{p} + K_2\dot{\boldsymbol{p}} \tag{5}$$

This means the uncertain term $\boldsymbol{\Delta}$ can be suppressed by the high gain of $K_a$. However, the high-gain AFC at least has the following three disadvantages.

1) Sometimes, the functions $f(\cdot,\cdot)$ and $g(\cdot,\cdot)$ can be identified exactly (or partly), and therefore, it is much better to design a controller based on them, and the AFC is only to attenuate $\boldsymbol{\Delta}$. But the AFC of (2) rejects both known nonlinearity and unknown uncertainty, which might result in that the condition of (4) is not easy to be satisfied.

2) Controller (2) will introduce an algebraic loop, i.e., the acceleration measurement is multiplied by the high-gain of $K_a$ and directly fed back into the system input $\boldsymbol{u}$, which might cause instability problem and deteriorate the closed loop performance greatly.

3) Controller (2) can only be applied to "fullactuated" plants, and there is no way to design $K_a$ for underactuated systems.

## 2 New AFC for fullactuated dynamics

In this section, we will present a new method for AFC design to overcome the first two disadvantages mentioned above. First, we rewrite (1) as

$$\ddot{\boldsymbol{p}} = f_n(\boldsymbol{p},\dot{\boldsymbol{p}}) + g_n(\boldsymbol{p},\dot{\boldsymbol{p}})\boldsymbol{u} + \bar{\boldsymbol{\Delta}} \tag{6}$$

where $f_n(\boldsymbol{p},\dot{\boldsymbol{p}})$ and $g_n(\boldsymbol{p},\dot{\boldsymbol{p}})$ are known functions with $g_n(\boldsymbol{p},\dot{\boldsymbol{p}})$ being reversible (this is reasonable because $g_n(\boldsymbol{p},\dot{\boldsymbol{p}})$ is often constant square matrix in reality), and

$$\bar{\boldsymbol{\Delta}} = \boldsymbol{\Delta} + [f(\boldsymbol{p},\dot{\boldsymbol{p}}) - f_n(\boldsymbol{p},\dot{\boldsymbol{p}})] + [g(\boldsymbol{p},\dot{\boldsymbol{p}}) - g_n(\boldsymbol{p},\dot{\boldsymbol{p}})]\boldsymbol{u} \tag{7}$$

is the uncertainty term.

Suppose

$$\boldsymbol{u} = k(\boldsymbol{p},\dot{\boldsymbol{p}}) \tag{8}$$

is a nominal stable controller of system (6). Then, we can suppose a new variable $\boldsymbol{v}$ and design a new controller as

$$\boldsymbol{u} = k(\boldsymbol{p},\dot{\boldsymbol{p}}) + g_n^{-1}(\boldsymbol{p},\dot{\boldsymbol{p}})\boldsymbol{v} \tag{9}$$

The closed loop system can be rewritten as

$$\ddot{\boldsymbol{p}} = f_n(\boldsymbol{p},\dot{\boldsymbol{p}}) + g_n(\boldsymbol{p},\dot{\boldsymbol{p}})k(\boldsymbol{p},\dot{\boldsymbol{p}}) + (\bar{\boldsymbol{\Delta}} + \boldsymbol{v}) \tag{10}$$

From (6), it can be seen that the measurability of acceleration signals is equivalent to that of the uncertainties $\bar{\boldsymbol{\Delta}}$. Thus not selecting $\boldsymbol{v} = -\bar{\boldsymbol{\Delta}}$, we can precisely eliminate the influence of $\bar{\boldsymbol{\Delta}}$ on the system. Unfortunately, it is unallowable to directly select $\boldsymbol{v} = -\bar{\boldsymbol{\Delta}}$ because it is obtained based on acceleration signals which introduces an algebraic loop. However, we can define $\boldsymbol{v}$ as

$$\dot{\boldsymbol{v}} = -l\boldsymbol{v} - b\bar{\boldsymbol{\Delta}} \tag{11}$$

Thus, the following frequency domain description of $\bar{\boldsymbol{\Delta}}$ can be obtained.

$$\bar{\boldsymbol{\Delta}}(s) + \boldsymbol{v}(s) = \frac{s + (l - b)}{s + l}\bar{\boldsymbol{\Delta}}(s) \tag{12}$$

Assume that $l \geq b > 0$. Thus, (12) is a high-pass filter. Because the acceleration, not the disturbance itself, is the measurable signal, $\bar{\boldsymbol{\Delta}}$ can be denoted as

$$\bar{\boldsymbol{\Delta}} = \ddot{\boldsymbol{p}} - f_n(\boldsymbol{p},\dot{\boldsymbol{p}}) - g_n(\boldsymbol{p},\dot{\boldsymbol{p}})\boldsymbol{u} \tag{13}$$

By substituting (9) and (13) into (11), the whole controller can be denoted as

$$\begin{aligned}&\dot{\boldsymbol{v}} = -(l-b)\boldsymbol{v} - b\{\ddot{\boldsymbol{p}} - f_n(\boldsymbol{p},\dot{\boldsymbol{p}}) - g_n(\boldsymbol{p},\dot{\boldsymbol{p}})k(\boldsymbol{p},\dot{\boldsymbol{p}})\}\\ &\boldsymbol{u} = k(\boldsymbol{p},\dot{\boldsymbol{p}}) - g_n^{-1}(\boldsymbol{p},\dot{\boldsymbol{p}})\boldsymbol{v}\end{aligned} \tag{14}$$

From (14), by adding the acceleration signals into the controller before a dynamic system (11), the algebraic loop is eliminated. Controller (14) is composed of two parts, wherein $\boldsymbol{u} = k(\boldsymbol{p},\dot{\boldsymbol{p}})$ makes the closed loop system satisfy some required performance index, and (11), called prefilter, is used to attenuate disturbances.

In order to obtain better performance, we can design $\boldsymbol{u} = k(\boldsymbol{p},\dot{\boldsymbol{p}})$ as a nonlinear $H_\infty$ controller, which has gained great development in recent years by using the Hamilton-Jacobi-Issacs (HJI) inequality and passivity analysis method[20−22].

To introduce the idea of $H_\infty$ control, consider the following affine nonlinear closed loop system.

$$\begin{aligned}&\dot{\boldsymbol{x}} = F(\boldsymbol{x}) + G(\boldsymbol{x})\boldsymbol{\omega}\\ &\boldsymbol{y} = H(\boldsymbol{x})\end{aligned} \tag{15}$$

where $\boldsymbol{x}$ is state; $\boldsymbol{\omega}$ is disturbance; $\boldsymbol{y}$ is output; $F(\cdot)$, $G(\cdot)$, and $H(\cdot)$ are all smooth functions. The following inequality is used as a design index for the nonlinear $H_\infty$ control.

$$\int_0^t \|\boldsymbol{y}(t)\|^2 \mathrm{d}\tau \leq \gamma^2 \int_0^t \|\boldsymbol{\omega}(t)\|^2 \mathrm{d}\tau \tag{16}$$

System (15) has an $L_2$-gain less than or equal to $\gamma$, if inequality (16) is satisfied for all $t \geq 0$ and $\boldsymbol{\omega} \in L_2[0,t]$. From [20], inequality (16) is satisfied if there is a smooth solution $V(\boldsymbol{x}) \geq 0$ such that the following HJI inequality

$$\frac{\partial V}{\partial \boldsymbol{x}}F(\boldsymbol{x}) + \frac{1}{4\gamma^2}\frac{\partial V}{\partial \boldsymbol{x}}G(\boldsymbol{x})G^{\mathrm{T}}(\boldsymbol{x})(\frac{\partial V}{\partial \boldsymbol{x}})^{\mathrm{T}} + H^{\mathrm{T}}(\boldsymbol{x})H(\boldsymbol{x}) \leq 0 \tag{17}$$

It is clear that if $k(\boldsymbol{p},\dot{\boldsymbol{p}})$ in (14) satisfies the following inequality.

$$\begin{aligned}&\frac{\partial V_0}{\partial \boldsymbol{p}}\dot{\boldsymbol{p}} + \frac{1}{4\gamma^2}\frac{\partial V_0}{\partial \dot{\boldsymbol{p}}}[f(\boldsymbol{p},\dot{\boldsymbol{p}}) + g(\boldsymbol{p},\dot{\boldsymbol{p}})k(\boldsymbol{p},\dot{\boldsymbol{p}})] + \frac{1}{4\gamma^2}\frac{\partial V_0}{\partial \dot{\boldsymbol{p}}}\times\\ &(\frac{\partial V_0}{\partial \dot{\boldsymbol{p}}})^{\mathrm{T}} + q(\boldsymbol{p},\dot{\boldsymbol{p}}) \leq 0\end{aligned} \tag{18}$$

where $V_0(\boldsymbol{p},\dot{\boldsymbol{p}})$ is a semipositive definition function and $q(\boldsymbol{p},\dot{\boldsymbol{p}})$ is a positive definition function such that $q(\boldsymbol{p},\dot{\boldsymbol{p}}) = 0$ if and only if $\boldsymbol{p} = \boldsymbol{0}$ and $\dot{\boldsymbol{p}} = \boldsymbol{0}$, then a controller with the performance of both the finite gain $L_2$ stable from disturbances to outputs and the frequency domain filtering through the linear prefilter can be obtained.

**Remark 1.** Up to now, the proposed AFC is redesigned to dedicate to the rejection of $\bar{\boldsymbol{\Delta}}$ instead of all of the nonlinear terms like in (2)∼(3), while eliminating algebraic loop. That means the disadvantages 1) and 2) of normal high gain

AFC have been overcome by the proposed control while the uncertainty rejection performance is maintanied. It should be noted that the new AFC method is a robust enhancement to a normal control, i.e., it can be combined with other robust controllers (for example, the nonlinear $H_\infty$ control) to reduce their conservativeness.

## 3 AFC for underactuated dynamics

Many underactuated vehicles can be modeled as the following "strict-feedback" system by coordinate transformation or ignoring some coupling terms[2−3, 5, 7].

$$\begin{aligned}\ddot{\boldsymbol{p}}_1 =& f_1(\boldsymbol{p}_1,\dot{\boldsymbol{p}}_1) + g_1(\boldsymbol{p}_1,\dot{\boldsymbol{p}}_1)\boldsymbol{p}_2 + h_1(\boldsymbol{p}_1,\dot{\boldsymbol{p}}_1)\boldsymbol{\Delta}_1\\ \ddot{\boldsymbol{p}}_2 =& f_2(\boldsymbol{p}_1,\dot{\boldsymbol{p}}_1,\boldsymbol{p}_2,\dot{\boldsymbol{p}}_2) + g_2(\boldsymbol{p}_1,\dot{\boldsymbol{p}}_1,\boldsymbol{p}_2,\dot{\boldsymbol{p}}_2)\boldsymbol{p}_3+\\ & h_2(\boldsymbol{p}_1,\dot{\boldsymbol{p}}_1,\boldsymbol{p}_2,\dot{\boldsymbol{p}}_2)\boldsymbol{\Delta}_2 \\ & \cdots\cdots \\ \ddot{\boldsymbol{p}}_r =& f_r(\boldsymbol{p}_1,\dot{\boldsymbol{p}}_1,\cdots,\boldsymbol{p}_r,\dot{\boldsymbol{p}}_r) + g_r(\boldsymbol{p}_1,\dot{\boldsymbol{p}}_1,\cdots,\boldsymbol{p}_r,\dot{\boldsymbol{p}}_r)\boldsymbol{u}+\\ & h_r(\boldsymbol{p}_1,\dot{\boldsymbol{p}}_1,\cdots,\boldsymbol{p}_r,\dot{\boldsymbol{p}}_r)\boldsymbol{\Delta}_r\end{aligned} \tag{19}$$

where $\boldsymbol{p}_1,\boldsymbol{p}_2,\cdots,\boldsymbol{p}_r \in \mathbf{R}^n$ are generalized position vectors or position errors; $\boldsymbol{\Delta}_1,\boldsymbol{\Delta}_2,\cdots,\boldsymbol{\Delta}_r$ are disturbances and ignored/unknown items; $\boldsymbol{u} \in \mathbf{R}^m$, $m = n$, is the control input; $f_i(\cdot), g_i(\cdot)$, and $h_i(\cdot)(i = 1, 2, \cdots, r)$ are known smooth functions with $h_i(\cdot)$ being reversible.

In this section, AFC enhanced $H_\infty$ controller will be given by using the idea of "prefilter" in the preceding section. By supposing $r = 2$ in (19), the following theorem can be concluded.

**Theorem 1.** Consider the following nonlinear system with external disturbances

$$\ddot{\boldsymbol{p}}_1 = f_1(\boldsymbol{p}_1,\dot{\boldsymbol{p}}_1) + g_1(\boldsymbol{p}_1,\dot{\boldsymbol{p}}_1)\boldsymbol{p}_2 + h_1(\boldsymbol{p}_1,\dot{\boldsymbol{p}}_1)\boldsymbol{\Delta}_1 \tag{20}$$

$$\begin{aligned}\ddot{\boldsymbol{p}}_2 =& f_2(\boldsymbol{p}_1,\dot{\boldsymbol{p}}_1,\boldsymbol{p}_2,\dot{\boldsymbol{p}}_2) + g_2(\boldsymbol{p}_1,\dot{\boldsymbol{p}}_1,\boldsymbol{p}_2,\dot{\boldsymbol{p}}_2)\boldsymbol{u}+\\ & h_2(\boldsymbol{p}_1,\dot{\boldsymbol{p}}_1,\boldsymbol{p}_2,\dot{\boldsymbol{p}}_2)\boldsymbol{\Delta}_2\end{aligned} \tag{21}$$

If there is a control law $\boldsymbol{p}_2 = a_1(\boldsymbol{p}_1,\dot{\boldsymbol{p}}_1)$, the following inequality is satisfied

$$\begin{aligned}&\frac{\partial V_1}{\partial \boldsymbol{p}_1}\dot{\boldsymbol{p}}_1 + \frac{\partial V_1}{\partial \dot{\boldsymbol{p}}_1}[f_1(\boldsymbol{p}_1,\dot{\boldsymbol{p}}_1) + g_1(\boldsymbol{p}_1,\dot{\boldsymbol{p}}_1)a_1(\boldsymbol{p}_1,\dot{\boldsymbol{p}}_1)]+\\ &\frac{1}{4\gamma^2}\frac{\partial V_1}{\partial \dot{\boldsymbol{p}}_1}h_1(\boldsymbol{p}_1,\dot{\boldsymbol{p}}_1)h_1^{\mathrm{T}}(\boldsymbol{p}_1,\dot{\boldsymbol{p}}_1)(\frac{\partial V_1}{\partial \dot{\boldsymbol{p}}_1})^{\mathrm{T}} + q_1(\boldsymbol{p}_1,\dot{\boldsymbol{p}}_1) \le 0\end{aligned} \tag{22}$$

where $q_1(\boldsymbol{p}_1,\dot{\boldsymbol{p}}_1) = l^{\mathrm{T}}(\boldsymbol{p}_1,\dot{\boldsymbol{p}}_1)l(\boldsymbol{p}_1,\dot{\boldsymbol{p}}_1))$ and $V_1(\boldsymbol{p}_1,\dot{\boldsymbol{p}}_1)$ are nonnegative-definite functions, then there is a control law $a(\boldsymbol{p}_1,\dot{\boldsymbol{p}}_1,\boldsymbol{p}_2,\dot{\boldsymbol{p}}_2,\boldsymbol{v}_1,\dot{\boldsymbol{v}}_1,\ddot{\boldsymbol{v}}_1,\boldsymbol{v}_2)$ such that the following system

$$\begin{aligned}\ddot{\boldsymbol{p}}_1 =& f_1(\boldsymbol{p}_1,\dot{\boldsymbol{p}}_1) + g_1(\boldsymbol{p}_1,\dot{\boldsymbol{p}}_1)\boldsymbol{p}_2 + h_1(\boldsymbol{p}_1,\dot{\boldsymbol{p}}_1)(\boldsymbol{\Delta}_1 + \boldsymbol{v}_1)\\ \ddot{\boldsymbol{p}}_2 =& f_2(\boldsymbol{p}_1,\dot{\boldsymbol{p}}_1,\boldsymbol{p}_2,\dot{\boldsymbol{p}}_2) + g_2(\boldsymbol{p}_1,\dot{\boldsymbol{p}}_1,\boldsymbol{p}_2,\dot{\boldsymbol{p}}_2)\boldsymbol{u}+\\ & h_2(\boldsymbol{p}_1,\dot{\boldsymbol{p}}_1,\boldsymbol{p}_2,\dot{\boldsymbol{p}}_2)(\boldsymbol{\Delta}_2 + \boldsymbol{v}_2)\\ \boldsymbol{y} =& l(\boldsymbol{p}_1,\dot{\boldsymbol{p}}_1)\end{aligned} \tag{23}$$

has an $L_2$ gain less than or equal to $\gamma$, taking $(\boldsymbol{\Delta}_1 + \boldsymbol{v}_1)$ and $(\boldsymbol{\Delta}_2 + \boldsymbol{v}_2)$ as new disturbance signals.

**Proof.** Suppose $\boldsymbol{z}_1 = \boldsymbol{p}_2 - a_1(\boldsymbol{p}_1,\dot{\boldsymbol{p}}_1) - g_1^{-1}(\boldsymbol{p}_1,\dot{\boldsymbol{p}}_1)h_1(\boldsymbol{p}_1,\dot{\boldsymbol{p}}_1)\boldsymbol{v}_1$, then the following dynamics can be obtained.

$$\begin{aligned}\ddot{\boldsymbol{p}}_1 =& f_1(\boldsymbol{p}_1,\dot{\boldsymbol{p}}_1) + g_1(\boldsymbol{p}_1,\dot{\boldsymbol{p}}_1)[a_1(\boldsymbol{p}_1,\dot{\boldsymbol{p}}_1) + \boldsymbol{z}_1]+\\ & h_1(\boldsymbol{p}_1,\dot{\boldsymbol{p}}_1)(\boldsymbol{\Delta}_1 + \boldsymbol{v}_1)\\ \dot{\boldsymbol{z}}_1 =& \bar{f}_1(\boldsymbol{p}_1,\dot{\boldsymbol{p}}_1,\boldsymbol{z}_1,\boldsymbol{v}_1,\dot{\boldsymbol{v}}_1) + \dot{\boldsymbol{p}}_2 + \bar{h}_1(\boldsymbol{p}_1,\dot{\boldsymbol{p}}_1,\boldsymbol{v}_1)(\boldsymbol{\Delta}_1 + \boldsymbol{v}_1)\end{aligned} \tag{24}$$

where (in the following sections, we will denote $h_i(\cdot)$, $g_i(\cdot)$, and $h_i(\cdot)$ as $h_i$, $g_i$, and $h_i$, respectively.)

$$\bar{h}_1(\boldsymbol{p}_1,\dot{\boldsymbol{p}}_1,\boldsymbol{v}_1) = -\{\frac{\partial}{\partial \boldsymbol{p}_1}(g_1^{-1}h_1\boldsymbol{v}_1) + \frac{\partial a_1}{\partial \dot{\boldsymbol{p}}_1}\}h_1$$

$$\begin{aligned}&\bar{f}_1(\boldsymbol{p}_1,\dot{\boldsymbol{p}}_1,\boldsymbol{z}_1,\boldsymbol{v}_1,\dot{\boldsymbol{v}}_1) =\\ &-[\frac{\partial}{\partial \dot{\boldsymbol{p}}_1}(g_1^{-1}h_1\boldsymbol{v}_1) + \frac{\partial a_1}{\partial \dot{\boldsymbol{p}}_1}](f_1 + g_1\boldsymbol{p}_2)-\\ &[\frac{\partial}{\partial \boldsymbol{p}_1}(g_1^{-1}h_1\boldsymbol{v}_1) + \frac{\partial a_1}{\partial \boldsymbol{p}_1}]\dot{\boldsymbol{p}}_1 - g_1^{-1}h_1\dot{\boldsymbol{v}}_1 - \bar{h}_1\boldsymbol{v}_1\end{aligned}$$

Introduce a new value function candidate for system (24).

$$V_2(\boldsymbol{p}_1,\dot{\boldsymbol{p}}_1,\boldsymbol{z}_1) = V_1(\boldsymbol{p}_1,\dot{\boldsymbol{p}}_1) + 0.5\boldsymbol{z}_1^{\mathrm{T}}\boldsymbol{z}_1 \tag{25}$$

Then, we have

$$\begin{aligned}&\frac{\partial V_2}{\partial \boldsymbol{p}_1}\dot{\boldsymbol{p}}_1 + \frac{\partial V_2}{\partial \dot{\boldsymbol{p}}_1}(f_1 + g_1\boldsymbol{p}_2 - h_1\boldsymbol{v}) + \frac{\partial V_2}{\partial \boldsymbol{z}_1}(\bar{f}_1 + \dot{\boldsymbol{p}}_2)+\\ &\boldsymbol{z}_1^{\mathrm{T}}Q_1\boldsymbol{z}_1 + q_1 + \frac{1}{4\gamma^2}[\frac{\partial V_2}{\partial \dot{\boldsymbol{p}}_1}\frac{\partial V_2}{\boldsymbol{z}_1}]\begin{bmatrix} h_1\\ \bar{h}_1\end{bmatrix}[h_1^{\mathrm{T}}\bar{h}_1^{\mathrm{T}}]\times\\ &\begin{bmatrix}(\frac{\partial V_2}{\partial \dot{\boldsymbol{p}}_1})^{\mathrm{T}}\\ (\frac{\partial V_2}{\partial \boldsymbol{z}_1})^{\mathrm{T}}\end{bmatrix} \le \boldsymbol{z}_1^{\mathrm{T}}\{\bar{f}_1 + \dot{\boldsymbol{p}}_2 + Q_1\boldsymbol{z}_1+\\ &\frac{1}{4\gamma^2}[4\gamma^2g_1^{\mathrm{T}}(\frac{\partial V_1}{\partial \dot{\boldsymbol{p}}_1})^{\mathrm{T}} + 2\bar{h}_1\bar{h}_1^{\mathrm{T}}(\frac{\partial V_1}{\partial \dot{\boldsymbol{p}}_1})^{\mathrm{T}} + \bar{h}_1\bar{h}_1^{\mathrm{T}}\boldsymbol{z}_1]\}\end{aligned} \tag{26}$$

where $Q_1$ is a positive definite matrix.

Consider

$$\begin{aligned}\dot{\boldsymbol{p}}_2 =& \bar{a}_2(\boldsymbol{p}_1,\dot{\boldsymbol{p}}_1,\boldsymbol{z}_1,\boldsymbol{v}_1,\dot{\boldsymbol{v}}_1) =\\ & -\bar{f}_1 - Q_1\boldsymbol{z}_1-\\ & \frac{1}{4\gamma^2}[4\gamma^2g_1^{\mathrm{T}}(\frac{\partial V_1}{\partial \dot{\boldsymbol{p}}_1})^{\mathrm{T}} + 2\bar{h}_1h_1^{\mathrm{T}}(\frac{\partial V_1}{\partial \dot{\boldsymbol{p}}_1})^{\mathrm{T}} + \bar{h}_1\bar{h}_1^{\mathrm{T}}\boldsymbol{z}_1]\end{aligned} \tag{27}$$

then (26) can be made less than or equal to 0. Thus, we have obtained a virtual controller such that system (24) has an $L_2$-gain less than or equal to $\gamma$, with $l(\boldsymbol{p}_1,\dot{\boldsymbol{p}}_1)$ as outputs and $(\boldsymbol{\Delta}_1 + \boldsymbol{v}_1)$ as external disturbances.

Next, suppose there is another new variable $\boldsymbol{z}_2 = \dot{\boldsymbol{p}}_2 - \bar{a}_2$. Then, the system dynamics (20)∼(21) can be expressed as follows.

$$\begin{aligned}\ddot{\boldsymbol{p}}_1 =& f_1(\boldsymbol{p}_1,\dot{\boldsymbol{p}}_1) + g_1(\boldsymbol{p}_1,\dot{\boldsymbol{p}}_1)a_1(\boldsymbol{p}_1,\dot{\boldsymbol{p}}_1) + g_1(\boldsymbol{p}_1,\dot{\boldsymbol{p}}_1)\boldsymbol{z}_1+\\ & h_1(\boldsymbol{p}_1,\dot{\boldsymbol{p}}_1)(\boldsymbol{\Delta}_1 + \boldsymbol{v}_1)\\ \dot{\boldsymbol{z}}_1 =& \bar{f}_1(\boldsymbol{p}_1,\dot{\boldsymbol{p}}_1,\boldsymbol{z}_1,\boldsymbol{v}_1,\dot{\boldsymbol{v}}_1) + \bar{a}_2(\boldsymbol{p}_1,\dot{\boldsymbol{p}}_1,\boldsymbol{z}_1,\boldsymbol{v}_1,\dot{\boldsymbol{v}}_1) + \boldsymbol{z}_2+\\ & \bar{h}_1(\boldsymbol{p}_1,\dot{\boldsymbol{p}}_1,\boldsymbol{v}_1)(\boldsymbol{\Delta}_1 + \boldsymbol{v}_1)\\ \dot{\boldsymbol{z}}_2 =& \bar{f}_2(\boldsymbol{p}_1,\dot{\boldsymbol{p}}_1,\boldsymbol{z}_1,\boldsymbol{z}_2,\boldsymbol{v}_1,\dot{\boldsymbol{v}}_1,\ddot{\boldsymbol{v}}_1) + \bar{g}_2(\boldsymbol{p}_1,\dot{\boldsymbol{p}}_1,\boldsymbol{z}_1,\boldsymbol{z}_2)u+\\ & \bar{h}_2(\boldsymbol{p}_1,\dot{\boldsymbol{p}}_1,\boldsymbol{z}_1,\boldsymbol{v}_1,\dot{\boldsymbol{v}}_1)(\boldsymbol{\Delta}_1 + \boldsymbol{v}_1)+\\ & \bar{h}_3(\boldsymbol{p}_1,\dot{\boldsymbol{p}}_1,\boldsymbol{z}_1,\boldsymbol{z}_2)(\boldsymbol{\Delta}_2 + \boldsymbol{v}_2)\end{aligned} \tag{28}$$

where

$$\bar{h}_2(\boldsymbol{p}_1,\dot{\boldsymbol{p}}_1,\boldsymbol{z}_1,\boldsymbol{v}_1,\dot{\boldsymbol{v}}_1) = -\frac{\partial a_2}{\partial \dot{\boldsymbol{p}}_1}h_1$$

$$\bar{h}_3(\boldsymbol{p}_1,\dot{\boldsymbol{p}}_1,\boldsymbol{z}_1,\boldsymbol{z}_2) = h_2(\boldsymbol{p}_1,\dot{\boldsymbol{p}}_1,\boldsymbol{p}_2,\dot{\boldsymbol{p}}_2)$$

$$\begin{aligned}&\bar{f}_2(\boldsymbol{p}_1,\dot{\boldsymbol{p}}_1,\boldsymbol{z}_1,\boldsymbol{z}_2,\boldsymbol{v}_1,\dot{\boldsymbol{v}}_1,\ddot{\boldsymbol{v}}_1) = f_2 - \frac{\partial a_2}{\partial \boldsymbol{p}_1}\dot{\boldsymbol{p}}_1-\\ &\frac{\partial a_2}{\partial \dot{\boldsymbol{p}}_1}(f_1 + g_1\boldsymbol{p}_2) - \frac{\partial a_2}{\partial \boldsymbol{p}_2}\dot{\boldsymbol{p}}_2 - \frac{\partial a_2}{\partial \boldsymbol{v}_1}\dot{\boldsymbol{v}}_1 - \frac{\partial a_2}{\partial \dot{\boldsymbol{v}}_1}\ddot{\boldsymbol{v}}_1 - \bar{h}_2\boldsymbol{v}_1 - \bar{h}_3\boldsymbol{v}_2\end{aligned}$$

$$\bar{g}_2(\boldsymbol{p}_1,\dot{\boldsymbol{p}}_1,\boldsymbol{z}_1,\boldsymbol{z}_2) = g_2(\boldsymbol{p}_1,\dot{\boldsymbol{p}}_1,\boldsymbol{p}_2,\dot{\boldsymbol{p}}_2)$$

Introduce a new value function candidate for system (28), namely,

$$V_2(\boldsymbol{p}_1,\dot{\boldsymbol{p}}_1,\boldsymbol{z}_1) = V_1(\boldsymbol{p}_1,\dot{\boldsymbol{p}}_1) + 0.5\boldsymbol{z}_1^{\mathrm{T}}\boldsymbol{z}_1 + 0.5\boldsymbol{z}_2^{\mathrm{T}}\boldsymbol{z}_2 \quad (29)$$

By the similar analysis process, we can conclude that if we take

$$\begin{aligned}\boldsymbol{u} =&\bar{a}(\boldsymbol{p}_1,\dot{\boldsymbol{p}}_1,\boldsymbol{z}_1,\boldsymbol{z}_2,\boldsymbol{v}_1,\dot{\boldsymbol{v}}_1,\ddot{\boldsymbol{v}}_1,\boldsymbol{v}_2) = \\ &-\bar{g}_2^{-1}\{\bar{f}_2 + \boldsymbol{z}_1 + Q_2\boldsymbol{z}_2 + \frac{1}{4\gamma^2}[2\bar{h}_2h_1^{\mathrm{T}}(\frac{\partial V_1}{\partial\dot{\boldsymbol{p}}_1})^{\mathrm{T}} + \\ &\bar{h}_2\bar{h}_1^{\mathrm{T}}\boldsymbol{z}_1 + (\bar{h}_2\bar{h}_2^{\mathrm{T}} + \bar{h}_3\bar{h}_3^{\mathrm{T}})\boldsymbol{z}_2]\}\end{aligned} \quad (30)$$

then,

$$\begin{aligned}&\frac{\partial V_3}{\partial\boldsymbol{p}_1}\dot{\boldsymbol{p}}_1 + \frac{\partial V_3}{\partial\dot{\boldsymbol{p}}_1}[f_1 + g_1\boldsymbol{p}_2 - h_1\boldsymbol{v}_1] + \frac{\partial V_3}{\partial\boldsymbol{z}_1}[\bar{f}_1 + \bar{a}_2 + \boldsymbol{z}_2] + \\ &\frac{\partial V_3}{\partial\boldsymbol{z}_2}[\bar{f}_2 + \bar{g}_2\boldsymbol{u}] + q_1 + \boldsymbol{z}_1^{\mathrm{T}}Q_1\boldsymbol{z}_1 + \boldsymbol{z}_2^{\mathrm{T}}Q_2\boldsymbol{z}_2 + \\ &\frac{1}{4\gamma^2}\left[\begin{array}{ccc}\frac{\partial V_3}{\partial\dot{\boldsymbol{p}}_1} & \frac{\partial V_3}{\partial\boldsymbol{z}_1} & \frac{\partial V_3}{\partial\boldsymbol{z}_2}\end{array}\right]\times \\ &\left[\begin{array}{cc}h_1 & 0\\ \bar{h}_1 & 0\\ \bar{h}_2 & \bar{h}_3\end{array}\right]\left[\begin{array}{ccc}h_1^{\mathrm{T}} & \bar{h}_1^{\mathrm{T}} & \bar{h}_2^{\mathrm{T}}\\ 0 & 0 & \bar{h}_3^{\mathrm{T}}\end{array}\right]\left[\begin{array}{c}\frac{\partial V_3}{\partial\dot{\boldsymbol{p}}_1}^{\mathrm{T}}\\ \frac{\partial V_3}{\partial\boldsymbol{z}_1}^{\mathrm{T}}\\ \frac{\partial V_3}{\partial\boldsymbol{z}_2}^{\mathrm{T}}\end{array}\right] \le \\ &\boldsymbol{z}_2^{\mathrm{T}}\{\bar{f}_2 + \bar{g}_2\boldsymbol{u} + \boldsymbol{z}_1 + Q_2\boldsymbol{z}_2 + \frac{1}{4\gamma^2}[2\bar{h}_2h_1^{\mathrm{T}}(\frac{\partial V_1}{\partial\dot{\boldsymbol{p}}_1})^{\mathrm{T}} + \\ &2\bar{h}_2\bar{h}_1^{\mathrm{T}}z_1 + (\bar{h}_2\bar{h}_2^{\mathrm{T}} + \bar{h}_3\bar{h}_3^{\mathrm{T}})\boldsymbol{z}_2]\}\end{aligned} \quad (31)$$

is less than or equal to 0.

From (31), taking $l(\boldsymbol{p}_1,\dot{\boldsymbol{p}}_1)$ as outputs, and $(\boldsymbol{\Delta}_1+\boldsymbol{v}_1)$ and $(\boldsymbol{\Delta}_2+\boldsymbol{v}_2)$ as external disturbances, system (28) has an $L_2$ gain less than or equal to $\gamma$, which means that system (23) has the same $L_2$-gain. □

Using Theorem 1, we can further design $\boldsymbol{v}_1$ and $\boldsymbol{v}_2$ just like we have done in Section 2

$$\begin{aligned}&\boldsymbol{v}_1^{(3)} = -k_1\boldsymbol{v}_1 - k_2\dot{\boldsymbol{v}}_1 - k_3\ddot{\boldsymbol{v}}_1 - b_1\boldsymbol{\Delta}_1\\ &\boldsymbol{y} = \boldsymbol{v}_1 + \boldsymbol{\Delta}_1\\ &\dot{\boldsymbol{v}}_2 = -k_4\boldsymbol{v}_2 - b_2\boldsymbol{\Delta}_2\\ &\boldsymbol{y} = \boldsymbol{v}_2 + \boldsymbol{\Delta}_2\end{aligned} \quad (32)$$

The parameters $k_1, k_2, k_3, k_4, b_1$, and $b_2$ can be designed on the basis of the linear system theory to attenuate $\boldsymbol{\Delta}_1$ and $\boldsymbol{\Delta}_2$. Further, (32) can be rewritten as (33) by replacing $\boldsymbol{\Delta}_1$ and $\boldsymbol{\Delta}_2$ with $\ddot{\boldsymbol{p}}_1$ and $\ddot{\boldsymbol{p}}_2$.

$$\begin{aligned}\boldsymbol{v}_1^{(3)} =& -k_1\boldsymbol{v}_1 - k_2\dot{\boldsymbol{v}}_1 - k_3\ddot{\boldsymbol{v}}_1 - b_1h_1^{-1}(\ddot{\boldsymbol{p}}_1 - f_1 - g_1\boldsymbol{p}_2)\\ \dot{\boldsymbol{v}}_2 =& -k_4\boldsymbol{v}_2 - b_2h_2^{-1}\{\ddot{\boldsymbol{p}}_2 - f_2 + \bar{f}_2 + \boldsymbol{z}_1 + Q_2\boldsymbol{z}_2 + \\ &\frac{1}{4\gamma^2}[2\bar{h}_2h_1^{\mathrm{T}}(\frac{\partial V_1}{\partial\dot{\boldsymbol{p}}_1})^{\mathrm{T}} + 2\bar{h}_2\bar{h}_1^{\mathrm{T}}\boldsymbol{z}_1 + \\ &(\bar{h}_2\bar{h}_2^{\mathrm{T}} + \bar{h}_3\bar{h}_3^{\mathrm{T}})\boldsymbol{z}_2]\}\end{aligned} \quad (33)$$

For system (20), repeat the process when Theorem 1 and (32) is being proved to obtain a similar controller as

$$\boldsymbol{u} = a(\boldsymbol{p}_1,\dot{\boldsymbol{p}}_1,\cdots,\boldsymbol{p}_r,\dot{\boldsymbol{p}}_r,\boldsymbol{v}_1,\cdots,\boldsymbol{v}_1^{2r-2},\cdots,\boldsymbol{v}_r)$$

and the following prefilter:

$$\begin{aligned}\boldsymbol{v}_1^{2r-1} =& -k_{1,1}\boldsymbol{v}_1 - \cdots - k_{1,2r-1}\boldsymbol{v}_1^{2r-2} - b_1\boldsymbol{\Delta}_1\\ \boldsymbol{v}_2^{2r-3} =& -k_{2,1}\boldsymbol{v}_1 - \cdots - k_{2,2r-1}\boldsymbol{v}_1^{2r-4} - b_2\boldsymbol{\Delta}_2\\ &\vdots\\ \dot{\boldsymbol{v}}_r =& -k_{r,1}\boldsymbol{v}_1 - b_r\boldsymbol{\Delta}_r\end{aligned} \quad (34)$$

## 4 Simulations of AFC for helicopter trajectory tracking control

In this section, we apply the proposed AFC enhanced $H_\infty$ controller design method to design the trajectory tracking controller of an underactuated model helicopter.

### 4.1 Dynamics of model helicopter

The complete dynamics of a helicopter can be divided into two parts: aerodynamics and body dynamics. Usually, the aerodynamics are too complicated to be used for the purpose of control design[23−24]. So the helicopter dynamics are often considered as a rigid body incorporating simplified aero- and actuator dynamics. The motion equation of a model helicopter can be written as

$$\left[\begin{array}{c}\dot{\boldsymbol{p}}\\ \dot{\boldsymbol{v}}^p\\ \dot{\boldsymbol{\Theta}}\\ \dot{\boldsymbol{\omega}}^b\end{array}\right] = \left[\begin{array}{c}\boldsymbol{v}^p\\ \frac{1}{m}R\boldsymbol{f}^b\\ \Psi\boldsymbol{\omega}^b\\ J^{-1}(\boldsymbol{\tau}^b - \boldsymbol{\omega}^b\times J)\boldsymbol{\omega}^b\end{array}\right] \quad (35)$$

where $\boldsymbol{p}\in\mathbf{R}^3$ and $\boldsymbol{v}^p\in\mathbf{R}^3$ are the position and velocity vectors in inertia frame; $R$ satisfies $RR^{\mathrm{T}} = I_3$, and $\det(R) = 1$ is the rotation matrix of the body frame relative to the inertia frame; and $\boldsymbol{\omega}^b$ is the angular velocity vector. $\boldsymbol{\Theta} = [\phi\quad\theta\quad\psi]^{\mathrm{T}}$ is the Euler angle vector; $m$ and $J$ are the mass and inertia of the helicopter, respectively; $\Psi$ is the transformation matrix from angular velocity to angular position; and $\boldsymbol{f}^b$ and $\boldsymbol{\tau}^b$ are force and moment presented in body frame, including disturbance force and moment.

The aerodynamics can be considered as a lumped model consisting of main rotor, tail rotor, horizontal stabilizer, vertical stabilizer, and fuselage. For the purpose of simplification, most researchers design the controllers by only considering the aerodynamics of main rotor and tail rotor.

$$\begin{aligned}\boldsymbol{f}^b &= \left[\begin{array}{c}X_M\\ Y_M + Y_T\\ Z_M\end{array}\right] + R^{\mathrm{T}}\left[\begin{array}{c}0\\ 0\\ mg\end{array}\right] + \boldsymbol{\Delta}_1\\ \boldsymbol{\tau}^b &= \left[\begin{array}{c}L_M\\ M_M + M_T\\ N_M\end{array}\right] + \left[\begin{array}{c}Y_Mh_M + Z_My_M + Y_Th_T\\ -X_Mh_M + Z_Ml_M\\ -Y_Ml_M - Y_Tl_T\end{array}\right] + \boldsymbol{\Delta}_2\end{aligned} \quad (36)$$

where $X$, $Y$, $Z$ and $L$, $M$, $N$ are the forces and torques about the $x$, $y$, and $z$ axes in body frame, respectively; the subscripts $_M$ and $_T$ denote the main and tail rotors; $h_M$, $y_M$, $h_T$, $l_M$, and $l_T$ are some distance constants; and $\boldsymbol{\Delta}_1$ and $\boldsymbol{\Delta}_2$ denote the unmodeled aerodynamic uncertainties including the ignored horizontal stabilizer, vertical stabilizer, and fuselage, and exogenous disturbances such as the force and torque induced by air mass and wind. In [7], the aerodynamics were calculated as

$$\begin{aligned}
&X_M = -T_M \sin a_{1s}, Y_M = T_M \sin b_{1s}\\
&Z_M = -T_M \cos a_{1s} \cos b_{1s}, X_T = 0\\
&Y_T = -T_T, Z_T = 0, R_M = K_1 b_{1s} - Q_M \sin a_{1s}\\
&M_M = K_2 a_{1s} + Q_M \sin b_{1s}, N_M = -Q_M \cos a_{1s} \cos b_{1s}\\
&R_T = 0, M_T = -Q_T, N_T = 0, Q_M = C_{M1} T_M^{1.5} + C_{M2}\\
&Q_T = C_{T1} T_T^{1.5} + C_{T2}
\end{aligned} \tag{37}$$

where $a_{1s}$ and $b_{1s}$ are the longitudinal and lateral tilts of the tip path plane of the main rotor with respect to shaft, respectively; $T_M$ and $T_T$ are forces of main and tail rotors, respectively.

### 4.2 The AFC design

In our simulations, the AFC is designed according to (38) which is obtained by (37). This is intended to enlarge the difference between the reference model (to be used for AFC design) and the high-fidelity model (to be controlled by the AFC), which is often in the modeling of the helicopter. The performance of AFC can be demonstrated under a worse condition with enlarged model uncertainty.

$$\begin{aligned}
&X = X_M = -T_M \sin a_{1s}, Y = Y_M = T_M \sin b_{1s}\\
&Z = Z_M = -T_M \cos a_{1s} \cos b_{1s}\\
&L = L_M = S_{L1} b_{1s} + S_{L2} Q_M\\
&M = M_M + M_T = S_{M1} a_{1s} + S_{M2} T_M + S_{M3} Q_T\\
&N = N_M = S_{N1} Q_M + S_{N2} T_T, T_M = S_{T_M 1} \theta_M + S_{T_M 2}\\
&T_T = S_{T_T} \theta_T + S_{T_T 2}, Q_M = S_{Q_M 1} \theta_M + S_{Q_M 2}\\
&Q_T = S_{Q_T} \theta_T + S_{Q_T 2}
\end{aligned} \tag{38}$$

After ignoring the couplings between rolling moments and lateral acceleration[7], the dynamics equations (35) can be denoted as

$$\begin{aligned}
&\ddot{\boldsymbol{p}} = \frac{1}{m} R \begin{bmatrix} 0 & 0 & Z \end{bmatrix}^{\mathrm{T}} + \begin{bmatrix} 0 & 0 & g \end{bmatrix}^{\mathrm{T}} + \boldsymbol{\Delta}_1\\
&\dot{\boldsymbol{\Theta}} = \Psi \boldsymbol{\omega}^b\\
&\dot{\boldsymbol{\omega}}^b = J^{-1}(\boldsymbol{\tau}^b - \boldsymbol{\omega}^b \times J\boldsymbol{\omega}^b + \boldsymbol{\Delta}_2)
\end{aligned} \tag{39}$$

where $Z$ and $\boldsymbol{\tau}^b$ are inputs.

(39) can be rewritten as

$$\ddot{\boldsymbol{p}}_1 = \boldsymbol{p}_2 + \boldsymbol{\Delta}_1$$

$$\ddot{\boldsymbol{p}}_2 = f_2(\boldsymbol{p}_1, \dot{\boldsymbol{p}}_1, \boldsymbol{p}_2, \dot{\boldsymbol{p}}_2) + g_2(\boldsymbol{p}_1, \dot{\boldsymbol{p}}_1, \boldsymbol{p}_2, \dot{\boldsymbol{p}}_2)\boldsymbol{u} + h_2 \boldsymbol{\Delta}_2 \tag{40}$$

$$\ddot{\psi} = f_3(\boldsymbol{p}_2, \dot{\boldsymbol{p}}_2, \boldsymbol{\Theta}, \boldsymbol{\omega}) + g_3(\boldsymbol{p}_2, \dot{\boldsymbol{p}}_2, \boldsymbol{\Theta}, \boldsymbol{\omega})\boldsymbol{u} + h_3 \boldsymbol{\Delta}_2 \tag{41}$$

where

$$\boldsymbol{p}_1 = \boldsymbol{p}$$

$$\boldsymbol{p}_2 = \frac{1}{m} R \begin{bmatrix} 0 & 0 & Z \end{bmatrix}^{\mathrm{T}} + \begin{bmatrix} 0 & 0 & g \end{bmatrix}^{\mathrm{T}}$$

$$f_2(\boldsymbol{p}_1, \dot{\boldsymbol{p}}_1, \boldsymbol{p}_2, \dot{\boldsymbol{p}}_2) = \frac{2}{m} \dot{Z} R(\boldsymbol{\omega}^b \times \begin{bmatrix} 0\\ 0\\ 1 \end{bmatrix} + \frac{1}{m} Z R[\boldsymbol{\omega}^b \times (\boldsymbol{\omega}^b \times \begin{bmatrix} 0\\ 0\\ 1 \end{bmatrix})] - \frac{1}{m} Z R\{[J^{-1}(\boldsymbol{\omega}^b \times J\boldsymbol{\omega}^b)] \times \begin{bmatrix} 0\\ 0\\ 1 \end{bmatrix}\})$$

$$g_2(\boldsymbol{p}_1, \dot{\boldsymbol{p}}_1, \boldsymbol{p}_2, \dot{\boldsymbol{p}}_2) = \frac{1}{m} \begin{bmatrix} ZR\overline{J} & R \begin{bmatrix} 0\\ 0\\ 0 \end{bmatrix} \end{bmatrix}, h_2 = \frac{1}{m} ZR\overline{J}$$

$$f_3(\boldsymbol{p}_2, \dot{\boldsymbol{p}}_2, \boldsymbol{\Theta}, \boldsymbol{\omega}) = -\begin{bmatrix} 0 & \dfrac{\sin\phi}{\cos\theta} & \dfrac{\cos\phi}{\cos\theta} \end{bmatrix} J^{-1}(\boldsymbol{\omega}^b \times J\boldsymbol{\omega}^b) + \frac{q\dot{\phi}\cos\phi}{\cos\theta} + \frac{q\dot{\theta}\sin\theta\sin\phi}{\cos^2\theta} - \frac{r\dot{\phi}\sin\phi}{\cos\theta} + \frac{r\dot{\theta}\sin\theta\cos\phi}{\cos^2\theta}$$

$$g_3(\boldsymbol{p}_2, \dot{\boldsymbol{p}}_2, \boldsymbol{\Theta}, \boldsymbol{\omega}) = \begin{bmatrix} 0 & \dfrac{\sin\phi}{\cos\theta} & \dfrac{\cos\phi}{\cos\theta} \end{bmatrix} J^{-1}$$

$$\boldsymbol{u} = \begin{bmatrix} (\boldsymbol{\tau}^b)^{\mathrm{T}} & \ddot{Z} \end{bmatrix}^{\mathrm{T}}$$

And $\overline{J}$ satisfies

$$\bar{J}\boldsymbol{\Delta}_2 = J(\boldsymbol{\Delta}_2 \times \begin{bmatrix} 0\\ 0\\ 1 \end{bmatrix})$$

(40)~(41) have the form of (20), thus, the AFC enhanced $\boldsymbol{H}_\infty$ controller of them can be designed. The trajectory tracking controller of the helicopter can be divided into the following 4 steps.

**Step 1.** Design a nonlinear AFC enhanced $H_\infty$ controller with measurable disturbances of (40) as (30) in Section 3, i.e.,

$$g_2(\boldsymbol{p}_1, \dot{\boldsymbol{p}}_1, \boldsymbol{p}_2, \dot{\boldsymbol{p}}_2)\boldsymbol{u} = \boldsymbol{u}_1 = a(\boldsymbol{p}_1, \dot{\boldsymbol{p}}_1, \boldsymbol{p}_2, \dot{\boldsymbol{p}}_2, \boldsymbol{v}_1, \dot{\boldsymbol{v}}_1, \ddot{\boldsymbol{v}}_1, v_2) \tag{42}$$

**Step 2.** Design a nonlinear AFC enhanced $H_\infty$ controller with measurable disturbances of (41) as (14) in Section 2, i.e.,

$$g_3(\boldsymbol{p}_2, \dot{\boldsymbol{p}}_2, \boldsymbol{\Theta}, \boldsymbol{\omega})\boldsymbol{u} = u_2 = k(\boldsymbol{p}_1, \dot{\boldsymbol{p}}_1) + h(\boldsymbol{p}_1, \dot{\boldsymbol{p}}_1)\boldsymbol{v}_2 \tag{43}$$

**Step 3.** Design linear prefilters as (32), i.e.,

$$\begin{aligned}
&\boldsymbol{v}_1^{(3)} = -k_1 \boldsymbol{v}_1 - k_2 \dot{\boldsymbol{v}}_1 - k_3 \ddot{\boldsymbol{v}}_1 - b_1 \boldsymbol{\Delta}_1\\
&\dot{\boldsymbol{v}}_2 = -k_4 \boldsymbol{v}_2 - b_2 \boldsymbol{\Delta}_2
\end{aligned} \tag{44}$$

**Step 4.** Obtain the final controller

$$\boldsymbol{u} = \begin{bmatrix} g_2(\boldsymbol{p}_1, \dot{\boldsymbol{p}}_1, \boldsymbol{p}_2, \dot{\boldsymbol{p}}_2)\\ g_3(\boldsymbol{p}_2, \dot{\boldsymbol{p}}_2, \boldsymbol{\Theta}, \boldsymbol{\omega}) \end{bmatrix}^{-1} \begin{bmatrix} \boldsymbol{u}_1\\ u_2 \end{bmatrix} \tag{45}$$

### 4.3 Simulation results

In order to verify the performance of the proposed AFC design method, we use the high fidelity model presented in [25] as the controlled system. The controller is designed according to the simplified model denoted by (35), (36), and (38) with the parameters

$$\begin{aligned}
&S_{L1} = -65.0398, S_{L2} = -0.062, S_{M1} = 65.0398\\
&S_{M2} = -0.01, S_{M3} = -1, S_{N1} = -1, S_{N2} = 0.898\\
&S_{T_M 1} = 1777, S_{T_M 2} = 39.8, S_{T_T 1} = 106.2, S_{T_T 2} = 6.9\\
&S_{Q_M 1} = 95.6, S_{Q_M 2} = -1.8, S_{Q_T 1} = -3.9, S_{Q_T 2} = -0.03\\
&h_M = 0.234, y_M = 0, h_T = 0.062\\
&l_M = 0.01, l_T = 0.898, M = 9.502
\end{aligned} \tag{46}$$

The parameters in (42)~(44) are respectively selected as

$$\begin{aligned}
&\gamma = 50, Q_1 = 5I, Q_2 = 50I, k(\boldsymbol{p}_1, \dot{\boldsymbol{p}}_1) = -4\boldsymbol{p}_1 - 2.8\dot{\boldsymbol{p}}_1,\\
&q(\boldsymbol{p}_1, \dot{\boldsymbol{p}}_1) = -5\boldsymbol{p}_1^{\mathrm{T}}\boldsymbol{p}_1 - 6\dot{\boldsymbol{p}}_1^{\mathrm{T}}\dot{\boldsymbol{p}}_1\\
&V(\boldsymbol{p}_1, \dot{\boldsymbol{p}}_1) = 3.3125\boldsymbol{p}_1^{\mathrm{T}}\boldsymbol{p}_1 + 1.25\boldsymbol{p}_1^{\mathrm{T}}\dot{\boldsymbol{p}}_1 + 0.3905\dot{\boldsymbol{p}}_1^{\mathrm{T}}\dot{\boldsymbol{p}}_1
\end{aligned} \tag{47}$$

$$\begin{aligned}&\gamma = 50, k(\boldsymbol{p}_1, \dot{\boldsymbol{p}}_1) = -4\boldsymbol{p}_1 - 2.8\dot{\boldsymbol{p}}_1,\\ &q(\boldsymbol{p}_1, \dot{\boldsymbol{p}}_1) = -5\boldsymbol{p}_1^{\mathrm{T}}\boldsymbol{p}_1 - 6\dot{\boldsymbol{p}}_1^{\mathrm{T}}\dot{\boldsymbol{p}}_1\\ &V(\boldsymbol{p}_1, \dot{\boldsymbol{p}}_1) = 3.3125\boldsymbol{p}_1^{\mathrm{T}}\boldsymbol{p}_1 + 1.25\boldsymbol{p}_1^{\mathrm{T}}\dot{\boldsymbol{p}}_1 + 0.3905\dot{\boldsymbol{p}}_1^{\mathrm{T}}\dot{\boldsymbol{p}}_1\end{aligned} \tag{48}$$

$$\begin{aligned}k_1 = -125, k_2 = -75, k_3 = -15\\ k_4 = -125, k_5 = -10, k_6 = -10\end{aligned} \tag{49}$$

The helicopter is controlled to maneuver a step change from the initial states of $x_0 = y_0 = z_0 = 1.0\,\mathrm{m}$, $\phi_0 = \theta_0 = \psi_0 = 0.1\,\mathrm{rad}$ to $x = y = z = 0.0\,\mathrm{m}$, and $\psi = 0.0\,\mathrm{rad}$.

In order to demonstrate the good performance of the new controller, we compare the simulation results with the linearized controller in [7] whose designed poles are $-1.4 \pm 1.4283\mathrm{j}$, $-5$, $-5$, $-5$, and the direct $H_\infty$ controller, i.e., controller (42)$\sim$(45) without $v_1$ and $v_2$. Fig. 1 shows the situation while there is only the uncertainty because of model simplification. From Fig. 1, we can see that under the control of linearized controller and the direct $H_\infty$ controller, the model uncertainty causes a stable tracking error, which has been attenuated successfully by the control with AFC.

Fig. 2 shows the case that external force disturbances of 50N are abruptly occurring to the first (39) at every 20 s, i.e.,

$$\ddot{\boldsymbol{p}}_1 = \boldsymbol{p}_2 + g\boldsymbol{e}_3 + \boldsymbol{\Delta}_{1m} + \boldsymbol{\Delta}_{1d} \tag{50}$$

where $\boldsymbol{\Delta}_{1m}$ is the uncertainty because of model simplification and $\boldsymbol{\Delta}_{1d}$ is the external disturbance as

$$\boldsymbol{\Delta}_{1d} = \begin{cases} [0,0,0]^{\mathrm{T}} & t < 20\,\mathrm{s}\\ [50,0,0]^{\mathrm{T}} & 20\,\mathrm{s} \le t < 40\,\mathrm{s}\\ [50,50,0]^{\mathrm{T}} & 40\,\mathrm{s} \le t < 60\,\mathrm{s}\\ [50,50,50]^{\mathrm{T}} & t \ge 60\,\mathrm{s}\end{cases} \tag{51}$$

In Fig. 2, we can see that neither the linearized controller nor the direct $H_\infty$ controller can overcome the disturbance forces, and there are stable position errors. In contrast, the solid lines indicate that the errors are rejected by the proposed AFC enhanced $H_\infty$ controller. It should be noted that the offsets of $\phi$ and $\theta$ in Fig. 2 after the disturbance are necessary for the helicopter to resist them.

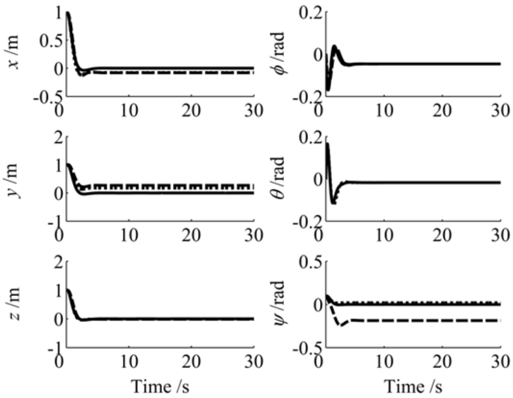


Fig. 1 AFC for model uncertainty rejection where the solid line is under the control with AFC enhanced $H_\infty$ controller (the dotted line is the $H_\infty$ controller, and the dashed line is the one with linearized controller)

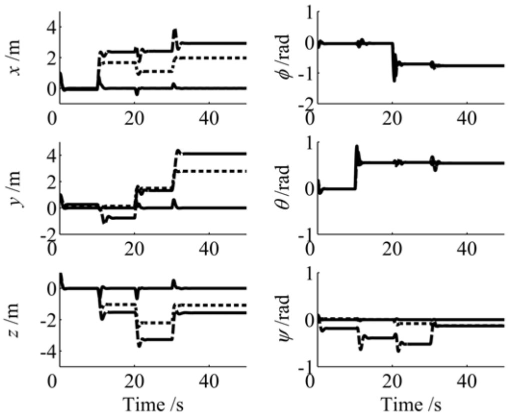


Fig. 2 AFC for both model uncertainty and external step-changed disturbance rejection

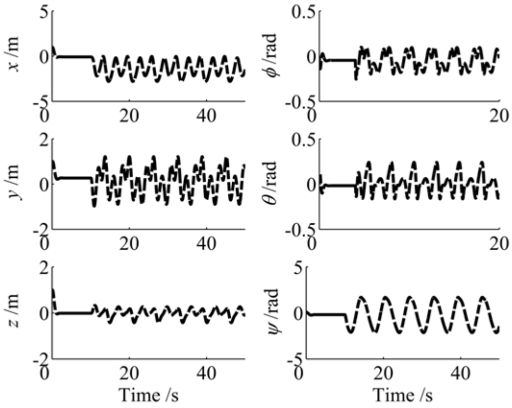


Fig. 3 Linearized controller for both model uncertainty and external sine-changed disturbance rejection

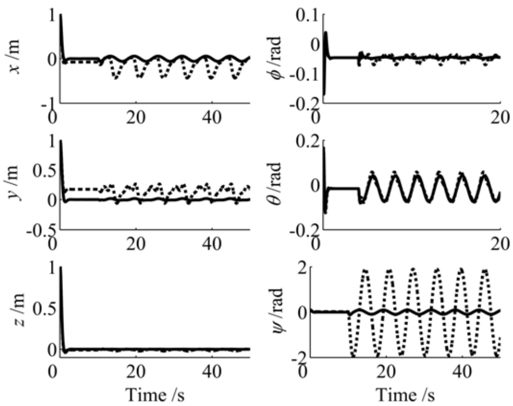


Fig. 4 AFC controller for both model uncertainty and external sine-changed disturbance rejection

Besides the step disturbance like (51), sine-changed torque disturbance is also tested, i.e.,

$$\boldsymbol{\Delta}_2 = \begin{cases} [0,0,0]^{\mathrm{T}} & t < 20\,\mathrm{s}\\ [A\sin\omega t, A\sin\omega t, A\sin\omega t]^{\mathrm{T}} & t \ge 20\,\mathrm{s}\end{cases} \tag{52}$$

where $A = 5$, and $\omega = 0.5$. The results are shown in Figs. 3 and 4, from which we can clearly see the improvement by the proposed AFC enhanced $H_\infty$ controller.

## 5 Conclusion

In this paper, we have presented a new AFC enhanced $H_\infty$ controller design approach for the uncertainties and external disturbances rejection of both fullactuated and underactuated dynamics. The AFC is designed as a robust enhancement to the normal control on the known dynamics by dedicating it to the rejection of unmodeled uncertainty. By using the concept of prefilter and backsteeping mechanism, the proposed AFC successfully overcomes the three disadvantages inherently seen in normal high-gain AFC. The simulation results with respect to the underactuated model helicopter show the improvements of the proposed method.

### References

1 Brunke S, Campbell M. Estimation architecture for future autonomous vehicles. In: Proceedings of American Control Conference. Alaska, USA: IEEE, 2002. 1108−1114

2 Frazzoli E, Dahlen M A, Feron E. Trajectory tracking control design for autonomous helicopters using a backstepping algorithm. In: Proceedings of American Control Conference. Chicago, USA: IEEE, 2000. 4102−4107

3 Do K D, Jiang Z P, Pan J, Nijmeijer H. A global output-feedback controller for stabilization and tracking of underactuated ODIN: a spherical underwater vehicle. *Automatica*, 2004, **40**(1): 117−124

4 Do K D, Jiang Z P, Pan J. Underactuated ship global tracking under relaxed conditions. *IEEE Transactions on Automatic Control*, 2002, **47**(9): 1529−1536

5 Repoulias F, Papadopoulos E. Trajectory planning and tracking control of underactuated AUVs. In: Proceedings of the 2005 IEEE International Conference on Robotics and Automation. Barcelona, Spain: IEEE, 2005. 1610−1615

6 Olfati-Sabe R. Nonlinear Control of Underactuated Mechanical Systems with Application to Robotics and Aerospace Vehicles [Ph. D. dissertation], Massachusetts Institute of Technology, 2001

7 Koo T J, Sastry S. Output tracking control design of a helicopter model based on approximated linearization. In: Proceedings of the 37th IEEE Conference on Decision and Control. Tampa, USA: IEEE, 1998. 3625−3640

8 Do K D, Pan J. Robust and adaptive path following for underactuated autonomous underwater vehicles. In: Proceedings of American Control Conference. Denver, USA: IEEE, 2003. 1994−1999

9 Lapierre L, Soetanto D, Pascoal A. Nonlinear path following with applications to the control of autonomous underwater vehicles. In: Proceedings of the 42nd IEEE Conference on Decision and Control. Denver, USA: IEEE, 2003. 1256−1261

10 Aguiar A P, Pascoal A M. Dynamic positioning and waypoint tracking of underactuated AUVs in the presence of ocean currents. In: Proceedings of the 41st IEEE Conference on Decision and Control. Las Vegas, USA: IEEE, 2002. 2105−2110

11 Yang Y S, Feng G, Ren J S. A combined backstepping and small-gain approach to robust adaptive fuzzy control for strick-feedback nonlinear systems. *IEEE Transactions on Systems, Man, and Cybernetics, Part A: Systems and Humans*, 2004, **34**(3): 406−420

12 Krishnamurthy P, Khorrami F. High-gain output-feedback control for nonlinear systems based on multiple time scaling. *Systems and Control Letters*, 2006, **56**(1): 7−15

13 Ding Z. Analysis and design of robust adaptive control for nonlinear output feedback systems under disturbances with unknown bounds. *IEE Proceedings on Control Theory and Applications*, 2000, **147**(6): 655−663

14 Pan Z G, Basar T. Adaptive controller design for tracking and disturbance attenuation in parametric strict-feedback nonlinear systems. *IEEE Transactions on Automatic Control*, 1998, **43**(8): 1066−1083

15 Xu W L, Han J D, Tso S K. Experimental study of contact transition control incorporating joint acceleration feedback. *IEEE/ASME Transactions on Mechatronics*, 2000, **5**(3): 292−301

16 Parsa K, Angeles J, Misra A K. Estimation of the flexural states of a macro-micro manipulator using acceleration data. In: Proceedings of IEEE International Conference on Robotics and Automation. Taipei, China: IEEE, 2003. 3120−3125

17 Han J D, Wang Y C, Tan D L, Xu W L. Acceleration feedback control for direct-drive motor system. In: Proceedings of IEEE International Conference on Intelligent Robots and Systems. Takamatsu, Japan: IEEE, 2000. 1068−1074

18 Vuilmet C. A MIMO backstepping control with acceleration feedback for torpedo. In: Proceedings of the 38th Southeastern Symposium on System Theory. Cookeville, USA: IEEE, 2006. 157−162

19 Kosuge K, Umetsu M, Furuta K. Robust linearization and control of robot arm using acceleration feedback. In: Proceedings of IEEE International Conference on Control and Application. Tokyo, Japan: IEEE, 1989. 161−165

20 Petersen I R, Anderson B D O, Jonckheere E A. A first principles solution to the non-singular $H_\infty$ control problem. *International Journal of Robust Nonlinear Control*, 1991, **1**(3): 171−185

21 Astrom K J. *Model Uncertainty and Robust Control*. Lund: Sweden COSY, 2000

22 Khalil H K. *Nonlinear Systems (Third Edition)*. New York: Prentice Hall, 2002

23 Leishman J G. *Principles of Helicopter Aerodynamics*. New York: Cambridge University Press, 2000

24 Padfield G D. *Helicopter Flight Dynamics: The Theory and Application of Flying Qualities and Simulation Modeling*. New York: American Institute of Aeronautics and Astronatics, 1996

25 Shim D H. Hierarchical Fight Control System Synthesis for Rotorcraft-based Unmanned Aerial Vehicles [Ph. D. dissertation], University of California, Berkeley, 2000

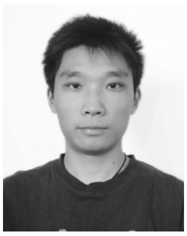

**HE Yu-Qing** Ph. D. candidate at State Key Laboratory of Robotics, Shenyang Institute of Automation, Chinese Academy of Sciences. His research interest covers nonlinear control, acceleration feedback based robust control, and predictive cotnrol. Corresponding author of this paper.
E-mail: heyuqing@sia.cn

**HAN Jian-Da** Professor at State Key Laboratory of Robotics, Shenyang Institute of Automation, Chinese Academy of Sciences. His research interest covers sensor based robot robust control system design, multi-robot system, and intelligent control system design.
E-mail: jdhan@sia.cn